

Studies on the Reaction Mechanism for Reductive Nitrosylation of Ferrihemoproteins in Buffer Solutions

Mikio Hoshino,*[†] Masahiro Maeda,[†] Reiko Konishi,[†] Hiroshi Seki,[†] and Peter C. Ford[‡]

Contribution from The Institute of Physical and Chemical Research, Wako, Saitama 351-01, Japan, and the Department of Chemistry, University of California, Santa Barbara, California 93106

Received September 28, 1995[⊗]

Abstract: Ferrihemoproteins in buffer solutions bind nitric oxide to yield their nitric oxide adducts. Reversible binding of NO was found for ferricytochrome *c* (Cyt^{III}) and metmyoglobin (Mb^{III}) at pH values lower than ca. 7.0. The equilibrium constants were obtained as $(1.6 \pm 0.1) \times 10^4 \text{ M}^{-1}$ for Cyt^{III} and $(1.3 \pm 0.1) \times 10^4 \text{ M}^{-1}$ for Mb^{III}. At higher pH, the reversible formation of the NO adducts is no longer observed; the NO adduct of Cyt^{III} (Cyt^{III}-NO) undergoes reduction to ferrocycytochrome *c*, Cyt^{II}, and that of Mb^{III} (Mb^{III}-NO) to the nitrosyl adduct of Mb^{II} (Mb^{II}-NO). Methemoglobin (Hb^{III}) reacts readily with NO even at pH < 6 to give the nitrosyl adduct of hemoglobin (Hb^{II}-NO). The rates for the formation of Cyt^{II}, Mb^{II}-NO, and Hb^{II}-NO were measured as functions of NO and OH⁻ concentrations. Kinetic analysis indicates that Cyt^{III}-NO and Mb^{III}-NO undergo nucleophilic attack by OH⁻ at higher pH to yield Cyt^{II} and Mb^{II}, respectively. Mb^{II} thus produced further reacts with NO to give Mb^{II}-NO. For Hb^{III}, the nitrosyl adduct (Hb^{III}-NO) was found to react with both OH⁻ and H₂O to give Hb^{II}-NO in the presence of excess NO. The rate constants for the reaction between the nitrosyl ferrihemoproteins and OH⁻ were determined as $(1.5 \pm 0.1) \times 10^3 \text{ M}^{-1} \text{ s}^{-1}$ for Cyt^{III}-NO, $(3.2 \pm 0.2) \times 10^2 \text{ M}^{-1} \text{ s}^{-1}$ for Mb^{III}-NO, and $(3.2 \pm 0.2) \times 10^3 \text{ M}^{-1} \text{ s}^{-1}$ for Hb^{III}-NO. The reductive nitrosylation of Hb^{III} observed at pH < 6.0 is explained by reaction of H₂O with Hb^{III}-NO: the rate constant is $(1.1 \pm 0.1) \times 10^{-3} \text{ s}^{-1}$.

Introduction

Nitric oxide has recently been recognized to have important physiological roles as a vascular regulator,^{1–5} in neuronal communication,^{6–9} and in nonspecific defense against bacterial infection by macrophages.^{10–13} It is produced *in vivo* from arginine by NO synthase in various organs.^{14–16} Hemoproteins are known to be very reactive toward NO to give the nitrosyl adducts,^{17,18} and this reactivity is now widely viewed as relevant to *in vivo* activity. Even before the biological importance of

nitric oxide was appreciated, NO interactions with metalloproteins were the subject of extensive studies.^{17,18} For example, paramagnetic adducts of NO with ferrihemoproteins had been probed by ESR spectroscopy,^{19–27} and various groups have investigated the photochemical reactivities of various nitrosyl metal porphyrins.^{28–33}

Recently, we described flash photolysis studies of nitrosyl complexes of ferri- and ferrohemoproteins in pH 6.5 aqueous

[†] The Institute of Physical and Chemical Research.

[‡] University of California.

[⊗] Abstract published in *Advance ACS Abstracts*, June 1, 1996.

(1) Reglinski, J.; Butler, A. R.; Glidewell, C. *Appl. Organomet. Chem.* **1994**, *8*, 25–31.

(2) Galla, H. J. *Angew. Chem.* **1993**, *32*, 378–380.

(3) Cullotta, E.; Koshland, D. E. *Science* **1992**, *258*, 1862–1865.

(4) Ignarro, L. J. *A. Rev. Pharmacol. Toxicol.* **1990**, *30*, 535–560.

(5) Moncada, S. M.; Palmer, R. M.; Higgs, E. A. *Biochem. Pharmacol.* **1989**, *38*, 1709–1713.

(6) Klatt, P.; Schmidt, K.; Uray, G.; Mayer, B. *J. Biol. Chem.* **1993**, *268*, 14781–14787.

(7) Shibuki, K.; Okada, D. *Nature* **1991**, *349*, 326–328.

(8) Bult, H.; Boeckxstaens, G. E.; Pelckmans, P. A.; Jordaens, F. H.; Van Maercke, Y. M.; Herman, A. G. *Nature* **1990**, *345*, 346–347.

(9) Bredt, D. S.; Hwang, P. M.; Glatt, C. E.; Lowenstein, C.; Reed, R. R.; Snyder, S. H. *Nature* **1991**, *351*, 714–718.

(10) Heck, D. E.; Laskin, D. L.; Gardener, C. R. *J. Biol. Chem.* **1992**, *267*, 21277–21280.

(11) Liew, F. Y.; Cox, F. E. G. *Immunol. Today* **1991**, *17*, A17–A21.

(12) Rubanyi, G. M.; Ho, E. H.; Cantor, E. H. *Biochim. Biophys. Res. Commun.* **1991**, *181*, 1392–1397.

(13) Hibbs, Jr., J. B.; Vavrin, Z.; Taintor, R. R. *J. Immunol.* **1987**, *138*, 550–565.

(14) Moncada, S.; Palmer, R. M. J.; Higgs, E. A. *Pharmacol. Rev.* **1991**, *43*, 109–142.

(15) Tayeh, M. a.; Marletta, M. A. *J. Biol. Chem.* **1989**, *264*, 19654–19658.

(16) Hibbs, J. B., Jr.; Taintor, R. R.; Vavrin, Z. *Science* **1987**, *235*, 473–476.

(17) Palmer, G. In *The Porphyrins*; Dolphin, D., Ed.; Academic Press: New York, 1979; Vol. IV, Part B, Chapter 6.

(18) Yonetani, T.; Yamamoto, H. In *Oxidases and Related Redox Systems*; King, T. E., Mason, S., Morrison, M., Eds.; University Park Press: Baltimore, MD, 1973; Vol. I, pp 278–298.

(19) Yonetani, T.; Yamamoto, H.; Erman, J. E.; Leigh, J. S., Jr.; Reed, G. H. *J. Biol. Chem.* **1972**, *247*, 2447–2455.

(20) Yoshimura, T.; Suzuki, S.; Nakahara, A.; Iwasaki, H.; Masuko, M.; Matsubara, T. *Biochemistry* **1986**, *25*, 2436–2442.

(21) Sharma, V. S.; Isaacson, R. A.; John, M. E.; Waterman, M. R.; Chevion, M. *Biochemistry* **1983**, *22*, 3897–3902.

(22) Trittelvitz, E.; Sick, H.; Gersonde, K. *Eur. J. Biochem.* **1972**, *31*, 578–584.

(23) Henry, Y.; Banerjee, R. *J. Mol. Biol.* **1973**, *73*, 469–482.

(24) LoBrutto, R.; Wei, Y.-H.; Yoshida, S.; Camp, H. L. V.; Scholes, C. P.; King, T. E. *Biophys. J.* **1984**, *45*, 473–479.

(25) Morse, R. H.; Chan, S. I. *J. Biol. Chem.* **1980**, *255*, 7876–7882.

(26) Boelens, R.; Rademaker, H.; Pel, R.; Wever, R. *Biochim. Biophys. Acta* **1982**, *679*, 84–94.

(27) Brudvig, G. W.; Stevens, T. H.; Chan, S. I. *Biochemistry* **1980**, *19*, 5275–5285.

(28) Hoshino, M.; Kogure, M. *J. Phys. Chem.* **1989**, *93*, 5478–5484.

(29) Cornelius, P. A.; Hochstrasser, R. M.; Steele, A. W. *J. Mol. Biol.* **1983**, *163*, 119–128.

(30) Hoffman, B. M.; Gibson, Q. H. *Proc. Natl. Acad. Sci. U.S.A.* **1978**, *75*, 21–25.

(31) Petrich, J. W.; Poyat, C.; Martin, J. L. *Biochemistry* **1988**, *27*, 4049.

(32) Traylor, T. G.; Madge, D.; Marsters, J.; Jongward, K.; Wu, G.-Z.; Waldes, K. *J. Am. Chem. Soc.* **1993**, *115*, 4808–4813.

(33) Hoshino, M.; Ozawa, K.; Seki, H.; Ford, P. C. *J. Am. Chem. Soc.* **1993**, *115*, 9568–9575.

solutions.³³ Among the ferrihemes, metmyoglobin, ferricytochrome *c*, and catalase were found to bind NO reversibly to give the respective nitrosyl adducts, but methemoglobin reacted with NO irreversibly to yield nitrosylhemoglobin. In the last case, the net reaction was reductive nitrosylation similar to earlier reports regarding NO reactions with certain iron(III) hemes.^{20,34–37} Despite those qualitative observations, quantitative studies of ferriheme protein reductive nitrosylations are lacking as is a substantiated unified reaction mechanism for this reaction which has potentially wide reaching implications regarding the interactions between metal centers and NO *in vivo*. The present work was undertaken to evaluate the detailed kinetics of the reductive nitrosylations of ferricytochrome *c*, metmyoglobin, and methemoglobin as a function of the medium.

Experimental Section

Ferricytochrome *c* (horse heart), methemoglobin (human), and metmyoglobin (whale skeletal muscle) were obtained from Sigma and were used as supplied. Nitric oxide gas (99.9%) was purchased from Takachiho Chemicals Inc. Co. The major impurities of the NO gas were N₂, CO₂, and N₂O. The pH values (pH 5–8) of phosphate buffer (ionic strength < 1.0) were adjusted with the use of the aqueous solutions of 0.067 M KH₂PO₄ and 0.067 M Na₂HPO₄. At pH higher than 8.0, the aqueous solutions of 0.10 M KH₂PO₄ and 0.05 M Na₂BO₄ were used.

A glass apparatus used for the present study consists of a round-bottomed vessel (50 mL), a quartz cell (1 cm optical path length), and a Teflon stopcock with a glass joint. A sample solution (10 mL) was pipetted into the vessel, and then the apparatus was fixed to a vacuum line with the glass joint.

All the sample solutions were prepared on the vacuum line with meticulous care in order to avoid oxygen contamination. After degassing the buffer solutions of ferrihemoproteins, NO was introduced into the solution via vacuum line techniques.³³ The total pressure (sum of *P*_{H₂O} plus *P*_{NO}) of the sample solution was measured by a mercury manometer. The concentration of NO dissolved in the sample solution was calculated from the partial pressure of NO with the use of the Bunsen coefficient of NO (4.71 × 10⁻² at 1 atm and 293 K).³⁸ It was assumed that the solubility of NO in the buffer solutions is the same as that in water.

Absorption spectra and the time profile of the absorbance changes at a given wavelength were recorded on a Hitachi 330 spectrophotometer. Kinetic data were treated according to the method of least squares.

The quantitative analysis of ionic products, NO₂⁻ and NO₃⁻, from the reductive nitrosylation of ferrihemoproteins was made by ion chromatography. An anion exchange column was mounted on an ion chromatographic analyzer (IC 100 from Yokogawa-Hokushin Electric Co. Ltd.) with the conductivity detector. The eluent was an equimolar mixture of 4 × 10⁻³ M Na₂CO₃ (4 cm³) and NaHCO₃ (4 cm³). The column pressure and the temperature used for analysis were, respectively, 50 kg/cm² and 40 °C.

Results

Ferricytochrome *c* (Cyt^{III}). Figure 1 shows the absorption spectra observed for Cyt^{III} in a pH 6.2 buffered solution under different NO pressures. The absorption maxima at 530 and 405 nm characteristic of Cyt^{III} decreased in intensity and new peaks appeared at 528, 580, and 410 nm as *P*_{NO} was increased. The spectral changes proved to be reversible: decreases in *P*_{NO} resulted in re-formation of Cyt^{III}, consistent with the following labile equilibrium:³³

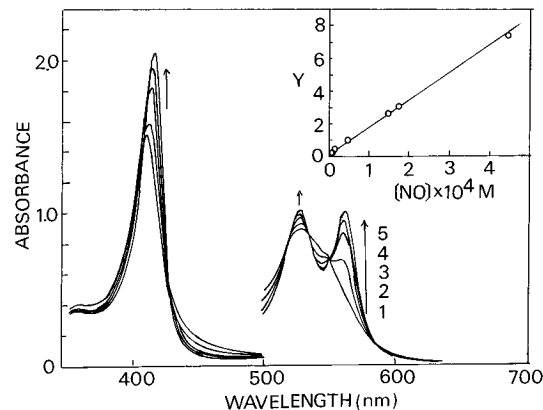
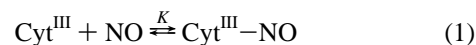


Figure 1. Absorption spectral changes of Cyt^{III} in a buffer solution at pH 6.1 in the presence of NO: (1) NO pressure (*P*_{NO}) 0 Torr; (2) *P*_{NO} = 27 Torr; (3) *P*_{NO} = 45 Torr; (4) *P*_{NO} = 95 Torr; (5) *P*_{NO} = 255 Torr. The concentration of Cyt^{III} is 1.6 × 10⁻⁵ M. The inset is the plot of *Y* vs the concentration of NO, obtained from the absorption spectral changes of Cyt^{III} in a buffer solution at pH 6.2 in the presence of NO (see the text).

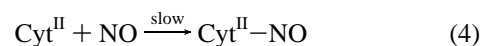
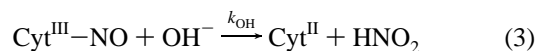


The equilibrium constant *K* was obtained from the spectral changes according to eq 2, where *D*(λ) is the absorbance of the solution at wavelength λ for a particular [NO] and *D*₀(λ) and

$$K[\text{NO}] = Y = [D(\lambda) - D_0(\lambda)]/[D_\infty(\lambda) - D(\lambda)] \quad (2)$$

*D*_∞(λ) are, respectively, the absorbances at [NO] = 0 and at “infinite” [NO]. The linear plot of *Y* vs [NO] obtained with the pH 6.2 buffer solution of Cyt^{III} is shown in Figure 1. From the slope of this plot, *K* was determined to be (1.6 ± 0.1) × 10⁴ M⁻¹.

At pH > 7.0, the spectral changes were no longer reversible; i.e., the Cyt^{III}–NO formed from Cyt^{III} and NO underwent further reaction. Figure 2 displays the time-dependent spectral changes observed for Cyt^{III} in a pH 8.5 buffer solution with *P*_{NO} = 100 Torr. The absorption bands characteristic of Cyt^{III}–NO disappeared and new bands appeared at 550, 520, and 420 nm over a period of minutes. The spectrum measured 20 min after initiation of the reaction was identical to that of authentic Cyt^{II}. This result indicates that Cyt^{III}–NO is transformed to Cyt^{II} at higher pH, a likely path being eq 3. It was found that Cyt^{II} reacts further with NO (eq 4), but this was very slow (data not shown) and was ignored in the kinetic analysis.



The kinetics for Cyt^{II} formation from Cyt^{III} plus NO according to eqs 1 and 3 can be formulated as follows:

$$[\text{Cyt}^{\text{II}}] = [\text{Cyt}^{\text{III}}]_0 [1 - \exp(-kt)] \quad (5)$$

where

$$[\text{Cyt}^{\text{III}}]_0 = [\text{Cyt}^{\text{III}}] + [\text{Cyt}^{\text{III}}-\text{NO}] + [\text{Cyt}^{\text{II}}] \quad (6)$$

and

$$k_{\text{obs}} = k_{\text{OH}}[\text{OH}^-]K[\text{NO}](1 + K[\text{NO}])^{-1} \quad (7)$$

The absorbance *D*(λ) at wavelength λ is

(34) Chien, J. C. W. *J. Am. Chem. Soc.* **1969**, *91*, 2166–2168.

(35) Ehrenberg, A.; Szczepkowski, T. W. *Acta Chem. Scand.* **1960**, *14*, 1684–1692.

(36) Keilin, D.; Hartree, E. F. *Nature* **1937**, *139*, 548.

(37) Wayland, B. B.; Olson, L. W. *J. Am. Chem. Soc.* **1974**, *96*, 6037–6041.

(38) *Kagakubinran*; Japan Chemical Society, Ed.; Maruzen: Tokyo, 1984; Vol. II, p 158.

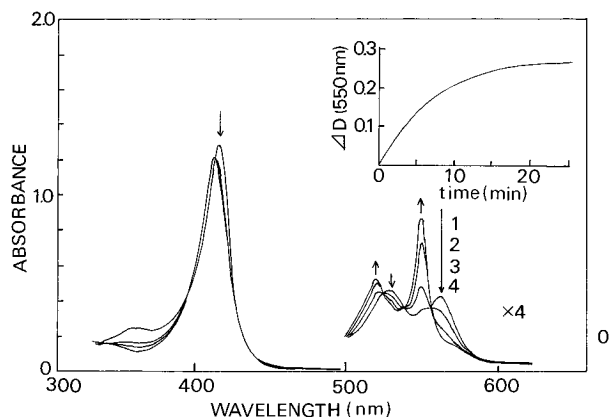


Figure 2. Time-dependent spectral changes of Cyt^{III}-NO at $P_{\text{NO}} = 132$ Torr in the buffer solution at pH 8.0: (1) before initiation of the reaction; (2) after 4 min; (3) after 15 min; (4) after 25 min. The inset shows the absorbance change measure at 550 nm as a function of time. The concentration of Cyt^{III} is 1.6×10^{-5} M.

$$D(\lambda) = \epsilon_{\text{III}}[\text{Cyt}^{\text{III}}] + \epsilon_{\text{NO}}[\text{Cyt}^{\text{III}}-\text{NO}] + \epsilon_{\text{II}}[\text{Cyt}^{\text{II}}] \quad (8)$$

with ϵ_{III} , ϵ_{NO} , and ϵ_{II} being, respectively, the absorption coefficients of Cyt^{III}, Cyt^{III}-NO, and Cyt^{II}. From these, the following equation is obtained:

$$D(\lambda) = D_{\infty}(\lambda) - B \exp(-kt) \quad (9)$$

where $D_{\infty}(\lambda)$ is the absorbance at an infinite time, i.e., equal to $\epsilon_{\text{II}}[\text{Cyt}^{\text{II}}]_0$ and

$$B = [\text{Cyt}^{\text{III}}]_0 \{ (\epsilon_{\text{II}} - \epsilon_{\text{III}}) + (\epsilon_{\text{II}} - \epsilon_{\text{NO}})K[\text{NO}] \} / (1 + K[\text{NO}]) \quad (10)$$

The time profile of the absorbance change ΔD (i.e., $D(\lambda) - D(\lambda)_0$, where $D(\lambda)_0$ is the absorbance at $t = 0$), at 550 nm is illustrated in Figure 2. ΔD gradually increases with time and levels off as predicted by eq 9. The rate constant k_{obs} was obtained from the slope of the linear plot of $\ln(D_{\infty}(\lambda) - D(\lambda))$ vs t .

The relationship between k_{obs} and $[\text{NO}]$ is illustrated in Figure 3. With increasing $[\text{NO}]$, k_{obs} asymptotically increases toward a limiting value, k_{lim} , of $4.0 \times 10^{-3} \text{ s}^{-1}$, where $k_{\text{lim}} = k_{\text{OH}}[\text{OH}^-]$ according to eq 7. It can be shown from the above equations that the relationship $k_{\text{lim}}(k_{\text{lim}} - k_{\text{obs}})^{-1} = 1 + K[\text{NO}]$ pertains. Consistent with this, the plot of $k_{\text{lim}}(k_{\text{lim}} - k_{\text{obs}})^{-1}$ vs $[\text{NO}]$ was linear with an intercept of 1.0. The slope of the line gave $K = (1.4 \pm 0.2) \times 10^4 \text{ M}^{-1}$, in good agreement with the value obtained from the spectral changes illustrated in Figures 1 and 2 for Cyt^{III} with various $[\text{NO}]$ in buffer solutions at pH 6.2.

The effects of pH on the rate constant k_{obs} were examined over the pH range 7.49–8.45 at $P_{\text{NO}} = 100 \pm 10$ Torr. Figure 4 displays a plot of k_{obs} as a function of hydroxide concentration. As predicted by eq 7, this is linear with a slope described by

$$\text{slope} = k_{\text{OH}}K[\text{NO}](1 + K[\text{NO}])^{-1} \quad (11)$$

From these data the bimolecular rate constant for the reaction between Cyt^{III}-NO and OH^- was determined to be $k_{\text{OH}} = (1.5 \pm 0.1) \times 10^3 \text{ M}^{-1} \text{ s}^{-1}$.

Metmyoglobin. Figure 5 shows the absorption spectra of metmyoglobin Mb^{III} under various P_{NO} . As P_{NO} increased, the absorption maxima at 631, 500, and 408 nm characteristic of Mb^{III} decreased in intensity and new bands appeared at 575, 535, and 417 nm. The spectral changes are reversible, indicating that the reaction is

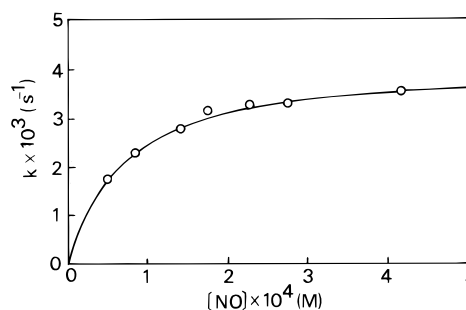


Figure 3. Rate constants k for the formation of Cyt^{II} from Cyt^{III}-NO at pH 8.35, represented as a function of NO concentration, $[\text{NO}]$. The solid line is calculated from eq 7 with the use of $k_{\infty} = k_{\text{OH}}[\text{OH}^-] = 4.0 \times 10^{-3} \text{ s}^{-1}$ and $K = 1.4 \times 10^4 \text{ M}^{-1}$.

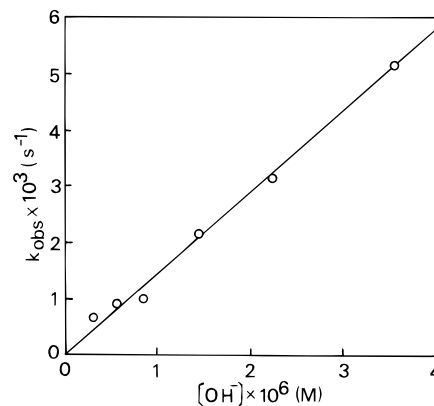


Figure 4. Rate constants k for the formation of Cyt^{II} from Cyt^{III}-NO at an NO pressure of 100 Torr, represented as a function of the concentration of OH^- ions.

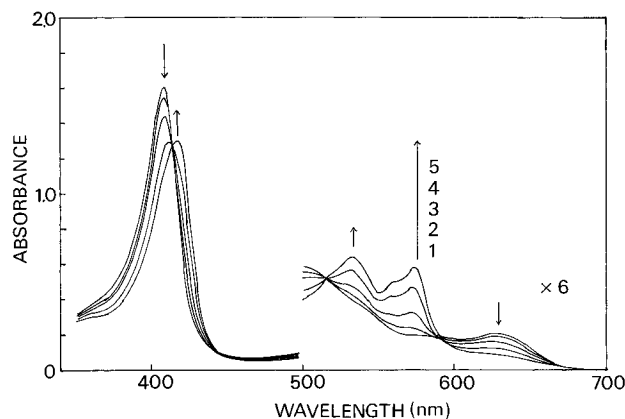
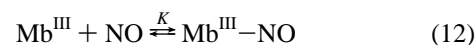


Figure 5. Absorption spectral changes of Mb^{III} in the buffer solution at pH 6.5 in the presence of NO: (1) NO pressure (P_{NO}) 0 Torr; (2) $P_{\text{NO}} = 19$ Torr; (3) $P_{\text{NO}} = 46$ Torr; (4) $P_{\text{NO}} = 100$ Torr; (5) $P_{\text{NO}} = 255$ Torr. The concentration of Mb^{III} is 1.0×10^{-5} M.

described as³³



From the spectral changes, the equilibrium constant of eq 12 was determined to be $(1.3 \pm 0.1) \times 10^4 \text{ M}^{-1}$, a value nearly identical to that obtained previously in unbuffered aqueous solution at pH 6.5 ($1.4 \times 10^4 \text{ M}^{-1}$).³³ The reversible reaction was observed over the pH range 6.0–7.2, and K was found to be independent of pH in the range studied.

For solution pH > 8.0, spectral changes for the reaction of Mb^{III} with NO were no longer reversible. Figure 6 shows the absorption spectra of Mb^{III} in a pH 8.79 buffer solution at $P_{\text{NO}} = 130$ Torr. The spectrum observed immediately after exposing

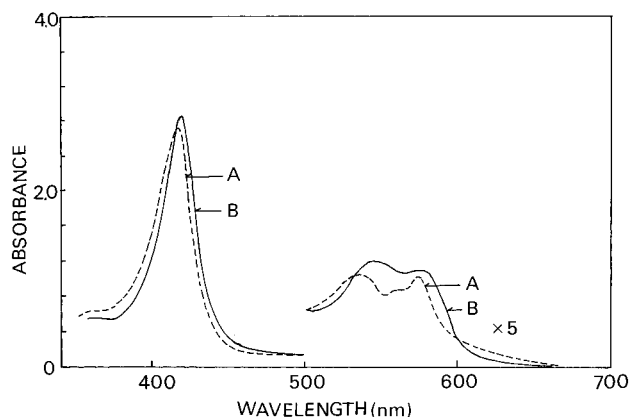
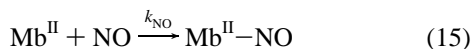
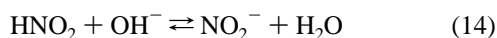
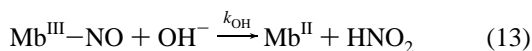


Figure 6. Absorption spectral change of Mb^{III}-NO in the buffer solution at pH 9: (A) before initiation of the reaction; (B) after 20 min. The NO pressure is 204 Torr: Spectrum B is in agreement with that of authentic Mb^{II}-NO. The concentration of Mb^{III} is 1.2×10^{-5} M.

the Mb^{III} solution to NO is that of Mb^{III}-NO. However, after 20 min, the spectrum was confirmed to be the same as that of authentic Mb^{II}-NO prepared directly from Mb^{II} plus NO. This suggests a sequence of reactions where Mb^{III}-NO reacts further with OH⁻ to give Mb^{II} (eq 13), which is then rapidly trapped by NO to give Mb^{II}-NO (eq 15). Free Mb^{II} was not detected spectroscopically, presumably because of the rapid reaction between Mb^{II} and excess NO ($k_{\text{NO}} = 1.7 \times 10^7 \text{ M}^{-1} \text{ s}^{-1}$).³³



The failure to observe Mb^{II} indicates the trapping by NO (eq 15) is very fast, so that rate-limiting step for Mb^{II} formation is eq 13. Therefore,

$$-d[\text{Mb}^{\text{II}}-\text{NO}]/dt = k_{\text{OH}}[\text{OH}^-][\text{Mb}^{\text{III}}-\text{NO}] = (k_{\text{OH}}K[\text{NO}]/(1 + K[\text{NO}])([\text{OH}^-])([\text{Mb}^{\text{III}}]_{\text{tot}} - [\text{Mb}^{\text{II}}-\text{NO}]) \quad (16)$$

where

$$[\text{Mb}^{\text{III}}]_{\text{tot}} = [\text{Mb}^{\text{III}}-\text{NO}] + [\text{Mb}^{\text{III}}] + [\text{Mb}^{\text{II}}-\text{NO}]$$

Thus, the rate for the formation of Mb^{II}-NO follows first-order kinetics, and the rate constant, k_{Mb} , has the same expression as eq 7:

$$k_{\text{Mb}} = k_{\text{OH}}'K[\text{NO}]/(1 + K[\text{NO}]) \quad (17)$$

where

$$k_{\text{OH}}' = k_{\text{OH}}[\text{OH}^-]$$

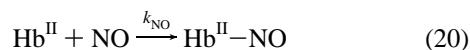
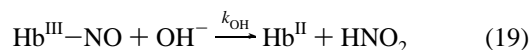
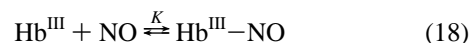
The value of k_{Mb} measured at a given pH higher than 8.3 asymptotically increases toward a limiting value with an increase in [NO]. The plot of $(k_{\text{Mb}})^{-1}$ vs $([\text{NO}])^{-1}$ gives a straight line. From the slope and intercept of the line, the values of k_{OH}' and K are determined. Surprisingly, the equilibrium constants K proved to be pH dependent, giving $(1.0 \pm 0.1) \times 10^3$, $(9 \pm 1) \times 10^2$, and $(6.2 \pm 0.5) \times 10^2 \text{ M}^{-1}$ at pH 8.3, 9.0, and 9.2, respectively. These are an order of magnitude smaller than those determined at lower pH by the spectroscopic titration method

which gave the value $(1.3 \pm 0.1) \times 10^4 \text{ M}^{-1}$ over the pH range 6.0–7.2 but a lower value, $(0.5 \pm 0.2) \times 10^4 \text{ M}^{-1}$, at pH 8.2.

The rate constants k_{OH}' were determined as $(8.8 \pm 0.2) \times 10^{-4}$, $(3.6 \pm 0.1) \times 10^{-3}$, and $(5.0 \pm 0.2) \times 10^{-3} \text{ s}^{-1}$ at pH 8.3, 9.0, and 9.2, respectively. The plot of k_{OH}' vs the concentration of OH⁻ gave a straight line with an intercept at the origin. The slope of the line gives $k_{\text{OH}} = (3.2 \pm 0.2) \times 10^2 \text{ M}^{-1} \text{ s}^{-1}$.

Equation 16 was derived on the assumption that the rate for the reaction between Mb^{II} and NO is much faster than that between Mb^{III}-NO and OH⁻. This can be rationalized by examining the pseudo-first-order rate constants for depletion and formation of Mb^{II} under the reaction conditions.³³ In this context, the reaction of Mb^{III} and NO in pH 8.79 buffer solutions was studied over the P_{NO} range 10–300 Torr. None of the uncomplexed form Mb^{II} could be detected even at a P_{NO} as low as 10 Torr. This was expected given that both k_{NO} ($1.7 \times 10^7 \text{ M}^{-1} \text{ s}^{-1}$) and K (ca. 10^{11} M^{-1}) for the reaction between Mb^{II} and NO are both much larger than those for the reaction between Mb^{III} and NO ($1.9 \times 10^5 \text{ M}^{-1} \text{ s}^{-1}$ and $1.3 \times 10^4 \text{ M}^{-1}$, respectively).³³

Methemoglobin. Absorption spectral changes of methemoglobin in the presence of NO were studied in buffer solution. The NO adduct of methemoglobin, Hb^{III}-NO, initially produced is gradually changed to Hb^{II}-NO even at pH 6.3. Spectral changes under NO ($P_{\text{NO}} = 10\text{--}300$ Torr) were not reversible, and the equilibrium constant for eq 18 could not be determined directly.



The spectrum of Hb^{III}-NO observed immediately after exposing the solution of Hb^{III} to 200 Torr of NO gas changes gradually to that of Hb^{II}-NO within 30 min. Hb^{II} was not detected under these conditions; thus, the mechanism for formation of Hb^{II}-NO appears to be analogous to that of Mb^{II}-NO formation from Mb^{III}-NO and OH⁻.

The equilibrium constant K in eq 18 and the rate constant k_{OH} can be obtained with the measurements of the rate constants k_{Hb} for the formation of Hb^{II}-NO as a function of [NO] at a given pH. On the assumption that eq 19 is the rate-determining step, k_{Hb} is given by $k_{\text{Hb}} = k_{\text{OH}}'K[\text{NO}]/(1 + K[\text{NO}])$. The plot of $(k_{\text{Hb}})^{-1}$ vs $([\text{NO}])^{-1}$ gave a straight line. From the slope and the intercept, K and k_{OH}' are obtained. The equilibrium constants are independent of pH in the range 5.6–7.4: $(1.4 \pm 0.1) \times 10^4$, $(1.4 \pm 0.1) \times 10^4$, $(1.2 \pm 0.1) \times 10^4$, and $(1.3 \pm 0.1) \times 10^4 \text{ M}^{-1}$ at pH = 5.6, 6.2, 7.1, and 7.4, respectively.

Figure 7 shows the plot of k_{OH}' as a function of [OH⁻]. Since the plot gives a straight line with a nonzero intercept, k_{OH}' is formulated as

$$k_{\text{OH}}' = k_{\text{OH}}[\text{OH}^-] + k_{\text{H}_2\text{O}} \quad (21)$$

The slope and the intercept of the line give $k_{\text{OH}} = 3.2 \times 10^3 \text{ M}^{-1} \text{ s}^{-1}$ and the pseudo-first-order rate constant, $k_{\text{H}_2\text{O}} = 1.1 \times 10^{-3} \text{ s}^{-1}$, respectively. The fact that the line has an intercept implies that Hb^{III}-NO reacts not only with OH⁻ but also with H₂O to yield Hb^{II}, which is subsequently transformed to Hb^{II}-NO by excess NO. Thus, the reductive nitrosylation of Hb^{III} observed at low pH is mainly ascribed to the following

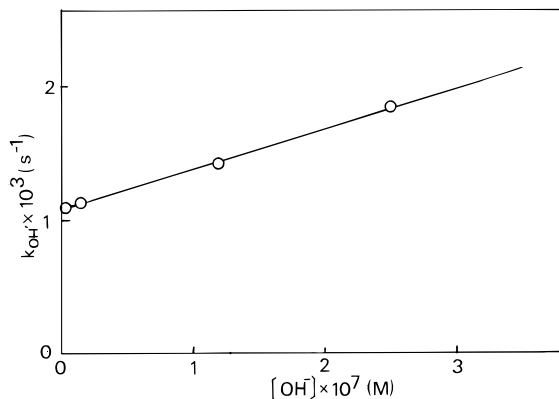
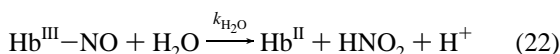


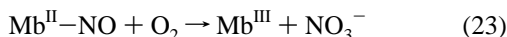
Figure 7. Rate constants $k_{OH'}$ for the reaction between $Hb^{III}-NO$ and OH^- , represented as a function of $[OH^-]$.

reaction:



With the increase in pH, eq 19 becomes a major reaction to yield Hb^{II} .

Detection of NO_2^- and NO_3^- . As mentioned above, reductive nitrosylation of ferriheme proteins should give nitrous acid or NO_2^- as the product. The ionic products were measured by ion chromatography. An aqueous solution (10 cm³) of 1.1×10^{-4} M Mb^{III} and 1.0×10^{-3} M Na_2CO_3 was degassed and exposed to NO gas at 120 Torr. The color of the solution instantaneously turned from brown to red. The formation of $Mb^{II}-NO$ in the solution was confirmed by absorption spectroscopy. After removing the excess NO, the solution was exposed to air. The products observed by chromatography of the aerated solution were 1.03×10^{-4} M NO_2^- and 0.81×10^{-4} M NO_3^- . The fact that the ratio $[NO_2^-]/[Mb^{III}]$ is approximately unity indicates that 1 mol of NO_2^- is produced from 1 mol of Mb^{III} by reductive nitrosylation. The formation of NO_3^- is readily explained by the air oxidation of $Mb^{II}-NO$:



The thermal oxidation of $Mb^{II}-NO$ shown in eq 23 has already been studied in detail.³⁹

Detection of NO_2^- and NO_3^- was carried out for an aqueous solution of 1.0×10^{-3} M Na_2CO_3 , which was exposed to NO gas at 200 Torr. After removal of NO gas, the aqueous solution was aerated. The concentrations of NO_2^- and NO_3^- detected in the aerated solution are far less than 10^{-6} M.

A quantitative analysis of NO_2^- and NO_3^- was also carried out for the aqueous solution of 1.0×10^{-4} M Cyt^{III} after exposure to NO gas at 120 Torr. The spectroscopic measurement revealed that the solution after removal of the excess NO contained 90% Cyt^{II} and 10% $Cyt^{II}-NO$. The aeration of this solution yields NO_2^- and NO_3^- : $[NO_2^-] + [NO_3^-] = 7.1 \times 10^{-5}$ M and $[NO_2^-]/[NO_3^-] = 0.4$. A similar study was carried out for the aqueous solution of 0.25×10^{-4} M Hb^{III} and 1.0×10^{-3} M Na_2CO_3 : $[NO_2^-] + [NO_3^-] = 1.24 \times 10^{-4}$ M and $[NO_2^-]/[NO_3^-] = 0.4$. These results are summarized as follows: (1) $[NO_2^-]$ is much smaller than the stoichiometric amount expected from the reductive nitrosylation reactions and (2) the amounts of $[NO_2^-] + [NO_3^-]$ detected here are ca. 30–40% less than those expected from the reductive nitrosylation reactions of Cyt^{III} and Hb^{III} and the subsequent air oxidation of $Cyt^{II}-NO$ and $Hb^{II}-NO$. It is suggested that, during the course

of air oxidation of $Cyt^{II}-NO$ and $Hb^{II}-NO$, NO_2^- produced by reductive nitrosylation is, in part, oxidized to NO_3^- . Such a complicated air oxidation reaction of $Cyt^{II}-NO$ and $Hb^{II}-NO$ would give a poor value for $[NO_2^-] + [NO_3^-]$ detected in the present system.

Discussion

Ferrihemoproteins Mb^{III} , Hb^{III} , and Cyt^{III} each reversibly bind NO in aqueous solution.³³ The central iron atom of Mb^{III} has the imidazole nitrogen of proximal histidine as the fifth ligand and H_2O as the sixth. As the water is readily replaced with other ligands, we assume that this represents the process leading to formation of $Mb^{III}-NO$. Similarly, the labile sixth iron site of Hb^{III} is readily available to formation of a Fe–NO bond. The reaction of Mb^{III} with NO is quite rapid ($k = 1.9 \times 10^5$ M⁻¹ s⁻¹) although slower than that for Mb^{II} .³³

In contrast, the axial coordination sites of Cyt^{III} are occupied by a methionine sulfur and the imidazole nitrogen of the proximal histidine,⁴⁰ one of which, presumably the methionine, is replaced by NO to give the nitrosyl complex. As we have reported, the reaction of Cyt^{III} with NO is several orders of magnitude slower ($k = 7.2 \times 10^2$ M⁻¹ s⁻¹)³³ than that of Mb^{III} although the equilibrium constants for complex formation are about the same. This suggests that the K values are dominated by the binding between NO and Fe(III) while the rate constants are influenced by other factors such as protein conformational changes. As noted in the Results, the reaction of Cyt^{II} with NO to form $Cyt^{II}-NO$ is even slower ($k = 8.3$ M⁻¹ s⁻¹)³³ than that for the ferric analogue Cyt^{III} , and it is for this reason that Cyt^{II} , not $Cyt^{II}-NO$, is the principal product of the NO reduction of Cyt^{II} under the conditions studied here. The axial coordination sites of the heme iron in Cyt^{II} are occupied by a methionine sulfur and an imidazole nitrogen, and the differences from Cyt^{III} are subtle, but it was argued that the oxidized form has a greater degree of heme exposure to the medium than the reduced form and that Fe–S bonding is weaker in the former.⁴⁰

In an earlier study³³ we reported equilibrium constants for the reaction of NO with ferrihemoproteins in unbuffered solutions to form the respective nitrosyl adducts. The studies described here were carried out in buffered solutions. The present data obtained for Cyt^{III} and Hb^{III} indicate little sensitivity of K to the presence of phosphate buffer or to pH. The equilibrium constant K for the reaction of Cyt^{III} with NO was determined to be $(1.6 \pm 0.2) \times 10^4$ M⁻¹ in pH 6.5 buffer solution, identical with that $(1.6 \times 10^4$ M⁻¹) obtained in a nonbuffered aqueous solution at pH 6.5.³³ At pH > 7.0, the subsequent reductive process was sufficiently rapid that it was necessary to obtain K from the kinetic analysis (i.e., eq 7). K determined in this manner for reaction of Cyt^{III} with NO at pH 8.5 was $(1.4 \pm 0.2) \times 10^4$ M⁻¹, within experimental uncertainty of that determined at pH 6.5.

A similar observation was made for formation of the NO adduct of Mb^{III} ; the spectroscopic titration of Mb^{III} with NO indicated that $K = (1.3 \pm 0.1) \times 10^4$ M⁻¹ in the pH range 6.13–7.2. The kinetic analysis for the reductive nitrosylation gave K values for the formation of $Mb^{III}-NO$ at pH ≥ 8.2 . The K values thus obtained at pH ≥ 8.2 are markedly smaller than those at pH ≤ 7.2 . This decrease in K was also observed by spectroscopic titration at pH 8.2. However, that value was prone to greater error owing to the rate of reductive nitrosylation. Although one might expect the acidity of H_2O in the axial site to affect K in this case, only about 14% of $Mb^{III}-H_2O$ would have been ionized at pH 8.2 according to the pK_a (8.99).⁴¹ This may suggest that the differences in K values between pH 7.2 and pH 8.2 are not ascribed to the ionization of the axial H_2O

(39) Anderson, H. J.; Skibsted, L. H. *J. Agric. Food Chem.* **1992**, *40*, 17041–1750.

(40) Takano, T.; Dickerson, R. E. *J. Mol. Biol.* **1981**, *153*, 95–115.

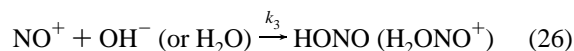
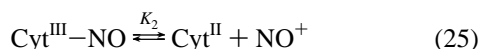
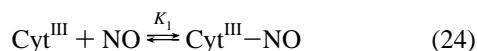
at higher pH. A possible interpretation could be a change in the conformation of the proteins surrounding heme in Mb^{III}-NO at pH > 7.5. Further study is necessary for full elucidation of the pH dependence of *K* values.

For Hb^{III}, the nitrosyl adduct is very unstable even at pH < 6.5, and reversible formation of Hb^{III}-NO was not detected. Thus, the determination of *K* values cannot be made by spectroscopic titration of Hb^{III} by NO. The kinetic analysis for the reductive nitrosylation of Hb^{III} afforded *K* = (1.3 ± 0.1) × 10⁴ M⁻¹ in the pH range 5.6–7.4.

The rate constants *k*_{OH} for the bimolecular reaction between nitrosylferrihememes and OH⁻ were determined to be 1.46 × 10³, 3.2 × 10², and 3.2 × 10³ M⁻¹ s⁻¹ for Cyt^{III}-NO, Mb^{III}-NO, and Hb^{III}-NO, respectively. The Hb^{III} undergoes reductive nitrosylation even at pH below 6.0, presumably because of a facile reaction with H₂O while Cyt^{III}-NO and Mb^{III}-NO react with H₂O much more slowly.

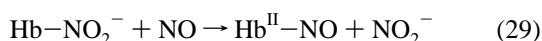
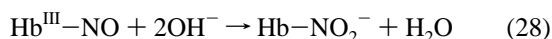
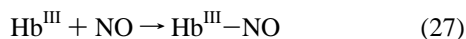
A few mechanisms have been proposed to explain reductive nitrosylation of ferrihemoproteins. One such proposal is that the NO adduct is reduced either intramolecularly or intermolecularly by the protein fragment surrounding the heme to give the nitrosyl adduct of the ferrohempoprotein.⁴²

Another proposal³⁵ is that the NO adduct of ferrihemoprotein thermally dissociates NO⁺ to give the ferrohempoprotein. The NO⁺ would react with OH⁻ (or another nucleophile), leaving ferrohempoproteins as a stable product or a product which reacts further with NO. This can be illustrated for Cyt^{III} as follows:



However, the only way in which this mechanism can display a rate law dependent on [OH⁻] would be for the rate of the back reaction of eq 25 (*k*₋₂) to be competitive with the trapping of NO⁺ by OH⁻ or H₂O. Since the rate for trapping of NO⁺ by H₂O (55 M) has been estimated to be extremely large (*k*₃ ≈ 10¹⁰ M⁻¹ s⁻¹),⁴³ even a diffusion-limited value for *k*₋₂ cannot be competitive with the hydrolysis of NO⁺ by solvent water. Thus, a mechanism occurring by spontaneous dissociation cannot explain the observed rate law.

The third proposed mechanism involves reaction of the ferriheme protein nitrosyl adduct with OH⁻ to give a nitroferroheme protein (or its conjugated acid).³⁴ Dissociation of nitrite ion (or nitrous acid) would give the ferroheme protein, and further reaction with NO would give the eventual nitrosyl ferroheme protein adducts.



This mechanism finds analogy with that proposed for the reversible hydrolysis of nitroprusside to give [Fe(CN)₅NO₂]⁴⁻ and in the hydrolysis of several ruthenium(II) nitrosyls.⁴⁴⁻⁴⁷

(41) Antonini, E.; Brunori, M. *Hemoglobin and Myoglobin in their Reactions with Ligands*; North-Holland: Amsterdam, 1971.

(42) Killday, K. B.; Tempesta, M. S.; Bailey, M. E.; Metral, C. J. *J. Agric. Food Chem.* **1988**, *36*, 909–914.

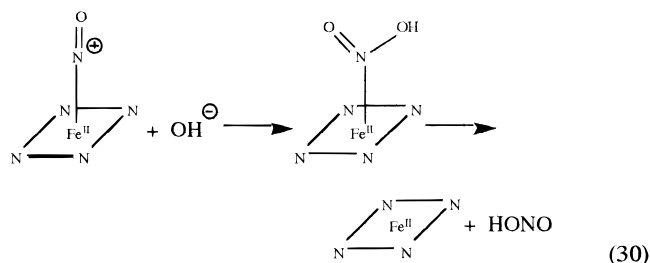
(43) Wolfe, S. K.; Swineheart, J. H. *Inorg. Chem.* **1975**, *14*, 1049–1053.

(44) Hofmann, K. A. *Justus Liebigs Ann. Chem.* **1900**, *312*, 1–33.

However, intermediate nitroferroheme proteins were not detected in the present study. This can easily be explained if the intermediate N-bound nitrous acid complex (and/or the conjugate base nitro complex) is labile toward dissociation under the reaction conditions. In that case, the rate-limiting step would be the reaction with OH⁻, a mechanism consistent with the rate law described in eq 17.

The reactivity of the ferriheme protein nitrosyl adducts is easily rationalized in terms of the charge transfer from the nitric oxide to the metal to give a linear structure best described electronically as Fe^{II}•••NO⁺. This makes the nitrosyl considerably more electrophilic, hence more susceptible to attack by hydroxide or another nucleophile. We do not have a ready explanation for the reactivity order characterized by the *k*_{OH} values, i.e., Hb^{III}-NO > Cyt^{III}-NO > Mb^{III}-NO, or for the much greater reactivity of Hb^{III}-NO toward H₂O. One consideration might be the Fe(III)/Fe(II) reduction potentials of these proteins, since the charge transfer might correlate with this parameter. However, while methemoglobin (*E*₀ = 0.144 V at pH 7) is a stronger oxidant than metmyoglobin (0.06 V), the same is not true for Cyt^{III} (0.22 V).⁴⁸ Clearly there are other factors which may also play a role.

The NO⁺ moiety is isoelectronic to carbon monoxide, and it is notable that a number of metal carbonyls (M-CO) are similarly susceptible to reaction with nucleophiles (such as OH⁻) to form nucleophile carbonyl adducts (such as M-C(O)OH⁻).⁴⁹ Loss of CO₂ plus H⁺ from the hydroxycarbonyl adduct leads to formal reduction of the metal center by two electrons rather than the formal one-electron process depicted by eq 30.



In summary, reductive nitrosylation of the ferrihemoproteins Cyt^{III}, Mb^{III}, and Hb^{III} first involves formation of the nitrosyl-ferrihemoprotein adducts. The coordinated NO of these species is activated toward nucleophilic attack by OH⁻ to give the ferrohempoproteins plus nitrite ion, presumably via the intermediacy of N-bonded NO₂⁻ or HONO. The ferrohempoproteins can react further with NO to give the respective nitrosyl complexes. The rate-limiting step of this sequence is apparently the reaction of the nitrosyl-ferriheme adducts with OH⁻. The rate constants *k*_{OH} vary in the order Hb^{III} > Cyt^{III} > Mb^{III}.

Acknowledgment. This work was supported by a grant on Solar Energy Conversion by Means of Photosynthesis from the Science and Technology Agency of Japan. P.C.F. acknowledges grants from the U.S. National Science Foundation (NSF CHE 9400919) and the U.S. Japan Cooperative Research (Photoconversion/Photosynthesis) Program (NSF INT 9116346).

JA953311W

(45) Rohdes, M. R.; Barley, M. H.; Meyer, T. J. *Inorg. Chem.* **1991**, *30*, 629–635.

(46) Barley, M. H.; Takeuchi, K. J.; Meyer, T. J. *J. Am. Chem. Soc.* **1986**, *108*, 5876–5885.

(47) Keene, F. R.; Salmon, D. J.; Meyer, T. J. *J. Am. Chem. Soc.* **1977**, *99*, 2384–2386.

(48) *Handbook of Biochemistry and Molecular Biology*; Fasman, G. D., Ed.; CRC Press: Cleveland, OH, 1975; pp 124–125.

(49) Ford, P. C.; Rokicki, A. *Adv. Organomet. Chem.* **1988**, *28*, 139–217.